RSC Advances

ROYAL SOCIETY OF CHEMISTRY

www.rsc.org/advances

Table of Contents

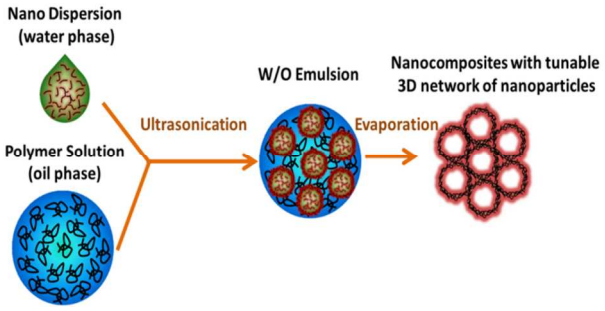

A facile and robust emulsion approach for fabrication of segregated polymeric nanocomposites with controllable nanoparticle dispersion/distribution is described.

RSC Advances

RSCPublishing

COMMUNICATION

Segregated Polymeric Nanocomposites wtih Tunable Three-dimensional Network of Nanoparticles by Controlling the Dispersion and Distribution

Cite this: DOI: 10.1039/x0xx00000x

Received xxxx,
Accepted xxxx

DOI: 10.1039/x0xx00000x

www.rsc.org/

Bing Geng,[ab⊥] Yu Wang,[b⊥] Bin Li[c] and Wei-Hong Zhong[*b]

A tunable three-dimensional network of nanoparticles was first time realized in a segregated polymeric nanocomposite via controlling the dispersion and distribution of nanoparticles in an emulsion system. The results show that the distribution of the nanofillers coupled with the porous structures can be effectively adjusted by simply varying the W/O ratio as well as the concentration of nanoparticles in the water phase. This study indicates a facile, cost-effective and universal emulsion process for fabrication of advanced polymeric nanocomposites with controlled distribution and dispersion of nanoparticles.

1. Introduction

It is well-known that, for nanocomposites, dispersion and distribution of nanoparticles (NPs) as well as the interfaces between NPs and polymer matrix are the most important factors controlling the final properties.[1-6] Besides a well dispersion of NPs, a controlled distribution of NPs will enable nanocomposites with unique properties, such as anisotropic conductivity,[7, 8] high electrical conductivity but low thermal conductivity for thermoelectric materials,[9, 10] high electrical conductivity and excellent elasticity with low density,[11] or improved adsorption and catalytic properties.[12] Unlike the methods for improvement of dispersion of NPs, control of distribution usually needs special manipulation of the interaction between NPs and polymer matrix as well as desired fabrication techniques. There are several strategies reported on control of distribution of NPs in nanocomposites, such as copolymer approach,[13] selective distribution of NPs in polymer blends with such as interpenetrating polymer network (IPN) structure,[14] and excluded-volume effects.[15]

Due to the unique morphology structures formed by the self-assembly of copolymers, the distribution of NPs has been successfully controlled in copolymer nanocomposites.[16-20] In order to “entrap” the NPs in a specific phase of

a copolymer, NPs are usually modified by structure-directing agents, which can preferentially interact with one of the blocks of the copolymer. Accompanying with the micro-phase separation of the block copolymer, the NPs are finally distributed in one of the phases of the copolymer nanocomposites. Selective distribution of NPs in polymer blends provides another effective way to control the distribution of NPs. For example, Yang and Liu et. al.[21, 22] found that carbon black can preferentially distribute in high density polyethylene (HDPE) when introduced into a HDPE/isotatic polypropylene (iPP) blend. By manipulating the phase structures of the blend, the distribution of NPs can be easily controlled. Similarly, distribution of NPs can also be controlled in blends with interpenetrating polymer networks (IPN) structure.[23-25] In these efforts, the precursor of NPs (such as the ions of metal particles) was introduced into the IPN system and only interacted with one of the networks, which has the functional groups acting as a transient anchoring agent. After the precursor was reduced by reduction agent, metal nanoparticles were *in situ* formed and distributed in one of the networks or at the interface. Recently, excluded-volume effects have also been employed to prepare nanocomposites with a controlled distribution of NPs. Usually, aqueous polymer emulsion[10, 26-28] or polymeric particles[29, 30] (ultra-high molecular weight polyethylene, for instance) were used as particles or cells creating excluded volume, which will finally localize the NPs at the interstitial space between polymer particles. Similarly, Ameli and Park et. al.[31-33] introduced supercritical CO_2 into nanofiller/PP composites to create excluded volume effects (the gas acts as the cell) and prepared nanocomposites with controllable distribution of nanofillers.

In this study, we report a facile, cost-effective, robust and universal method for fabrication of porous segregated nanocomposites with well-controlled distribution and dispersion of NPs (e.g. carbon nanotubes, CNTs,) based on emulsion technology. Via design of the compositions in the water phase (i.e., a homogeneous aqueous suspension of CNTs) as well as in the oil phase (polymer solution with organic solvent), a W/O emulsion system was prepared by ultrasonication for the fabrication of the nanocomposites. The CNTs in the water phase suspension can play the role of surfactant and results in a stable emulsion.[34-40] After the emulsion was cast and dried on a substrate (glass, for example), a porous nanocomposite film with controlled distribution and dispersion

of CNTs was obtained. It is believed that this is a scalable technology and can be easily commercialized, thus, will be significant for mass production of porous multi-functional nanocomposites.

2. Experimental

2.1 Materials.

The materials employed in this study include: Polycarbonate (PC) (SABIC Innovation Plastics), CNTs (diameter: 10 - 20 nm, length: 10 - 30 μm, Cheap Tubes Inc.), PEDOT:PSS aqueous solution (concentration: 1.13 wt%, high conductive grade, Sigma-Aldrich) and solvents (chloroform and DI water).

2.2 Sample preparation.

In the first step, the water phase was prepared by dispersing CNTs in aqueous solution of PEDOT:PSS by ultrasonication (20% amplitude for 5min with ice bath, Branson Digital Untrasonicator, Model 450). For masterbatch, the ratio between CNTs and PEDOT: PSS solution was fixed around 0.5 g : 10 mL. For the samples with different loading of NPs or different W/O ratio, the masterbatch of the nano-dispersion was diluted by DI water appropriately according to the calculation. At the same time, the oil phase, that is, the polymer solution (PC in chloroform, 5 wt%) was prepared in advance. In the second step, the well-dispersed CNT/PEDOT:PSS suspension (water phase) was added into the polymer solution (oil phase) and a W/O emulsion was obtained by ultrasonication of the mixture (Branson Digital Ultrasonicator, 20% amplitude, 3 min with ice bath). In the last step, the emulsion was cast on a glass substrate via a multiple clearance square applicator (Paul N. Gardner Company, INC). The thickness of the film was controlled by casting the emulsion with different gap values. After all the solvents (chloroform and water) evaporated at room temperature for about 10 min., a porous nanocomposite film with some residual water was obtained and further dried at 75 °C for 1 hour to completely remove the solvents before the electrical measurement.

2.3 Characterizations

The microstructures were characterized by Scanning electron microscopy (FEI Quanta 200F) and optical microscope. The surface contacted with the glass substrate was directly used for SEM observation. The fracture surface of the porous film was prepared by fracturing the film in liquid nitrogen. For optical image, the thinnest film with thickness of ca. 15 μm was used and the images were taken at room temperature by Olympus BX51. For electrical conductivity measurement, the resistance of the film was measured for 5 times for each sample by two-probe method at ambient temperatures using 2410 SourceMeter (KEITHLEY, Inc.) Then the conductivity was calculated by $\rho = RA/l$, where R is the resistance obtained from the measurement, A is the area of the section, l is the length of the sample used for the testing.

3. Results and Discussion

It is well-known that emulsion technology has been widely used for fabrication of porous materials.[40-43] However, to our knowledge, it is the first time to design the compositions in the water phase as well as the oil phase for the fabrication of porous nanocomposites. As illustrated in the Figure 1 (a), a well-dispersed NPs suspension (CNT treated by PEDOT:PSS and dispersed in DI water) as the water phase and a polymer solution (polycarbonate in chloroform) as the oil phase have been employed to form a W/O emulsion system. During ultrasonication, the NP suspension is broken into micro droplets. The compositions as well as the structures of the W/O system are further illustrated in Figure 1 (b). It is noted that the W/O emulsion system can be stable without surfactant due to the NPs in the water phase.[36, 44, 45] By casting the emulsion on a glass substrate, the solvents (chloroform for the oil phase and water for the water phase) are removed during evaporation and a porous nanocomposite can be obtained as shown Figure 1 (c). The porous structures are confirmed by the SEM images (Figure 1 (d) and (e)). Figure 1 (f) demonstrates the controlled distribution of CNTs in the porous nanocomposites. In brief, the design of the compositions in the water phase (nanoparticle suspension, for example) for the emulsion system provides a versatile, simple and effective approach to fabrication of nanocomposites, especially porous polymeric nanocomposites, with controlled distribution and dispersion of NPs. Theoretically, any two immiscible liquid phases can be used for constructing an emulsion system and the distribution of the components can be controlled

after the removing of the solvent. It is worth to pointing out that the flexibility in the design of the compositions in the two phases will enable programmable functionalities for nanocomposites.

To investigate how the structure affects the properties of the porous nanocomposites, the loading of CNTs has been changed from 0 to 6 wt% and the electrical conductivity has been measured. As displayed in Figure 2 (a), the electrical conductivity increases non-linearly with the loading of CNTs, similar to that for bulk conductive nanocomposites. However, it is noted that a very low percolation loading (< 0.06 vol.% or 0.3 wt%) has been obtained as indicated in Figure 2 (a). This percolation loading is much lower than that for common PC/CNT nanocomposites, which is usually well above 1 wt%.[46-48] The low threshold for percolation should be benefited from a controlled distribution and a good dispersion of CNTs in the porous composite film as illustrated by the cartoon in Figure 2 (a). Due to the fact that the nanotubes are trapped in the micro droplets, the final distribution of nanotubes is shaped by the dried droplets, that is, the pore structures. As long as the concentration of the droplets is high enough to construct a network, a network of conductive nanotubes will also form at the percolation point. This coupling effect is further confirmed by the optical images (Figure 2 (b) and Figure S1, Supporting Information) and SEM images (Figure 2 (c) and Figure S2, Supporting Information). From the optical images, a clear network of the pores can be observed. The SEM images distinctly show a distribution and a good dispersion of CNTs on the surface of the pores. The above findings indicate that the distribution and the dispersion of NPs can be effectively controlled by individual design of the compositions in the water or oil phase for the emulsion system.

Indeed, a significant finding as shown in Figure 3 is that the pore structures, that is, the distribution of CNTs, can be simply but effectively manipulated through the loading of the NPs, that is, the concentration of the NPs in the water-based suspension if a constant W/O was used. It was found that the diameter of the pores decreases dramatically with the increasing of the nanotube loadings when the loading is less than 1 wt% as shown by the SEM images and the statistical results of the pore size in Figure 3. It was also found that the pore size shows much less dependent behaviour on the loading of CNTs when the CNT loading is higher than 1 wt%, indicating that the

water droplet becomes stable when the concentration of CNTs in the droplet is higher than 0.3 wt% (the CNT concentration in the droplet for the sample with 1 wt% CNT in the final composite). These results should be related to the mechanism for the stability of the micro droplets of the nanotube suspension. Based on Figure 3, one can conclude that a higher concentration of NPs in the suspension (ca. 0.3 wt%) is helpful to stabilize the micro droplets and suppress the coalescence of micro droplets, which results in a smaller pore size. At the same time, it was found that the pore size increased slightly with the increasing of the thickness of the film (Figure S3, Supporting Information), which should be relevant to the fact that it takes more time for the thicker film to evaporate. These results once again confirm that CNTs can act as a surfactant for the emulsion. Meaningfully, the above finding indicates that the individual design of the compositions in water or oil phase will provide a very effective approach to fabricating porous nanocomposites with high concentration of functional NPs, which will find their significant applications into such as electrodes, sensors and catalytic films.

Another simple but effective way we can use to manipulate the distribution of NPs for the porous nanocomposite is to alter the W/O ratio. In this study, a volume ratio of the water phase (W) to the oil phase (O) ranged from 0.05 to 0.3 has been investigated. In order to evaluate the effects of W/O volume ratio on the structures and properties of the porous composite films, a constant overall loading of CNTs (2 wt%) was applied for all these samples. It is seen that the range of the volume ratio is primarily determined by the stability of the W/O system. As shown in Figure 4, it can be found that the W/O ratio has a profound influence on the structures and the properties of the porous nanocomposites. In specific, the pore size increases notably with the W/O ratio as shown in the optical images (Figure 4 (a) – (d)) and SEM images (Figure S4, Supporting Information). The explanation of this result is the same as that for the NPs loading dependent behaviour of the pore size, that is, a high concentration of NPs in the nano-dispersion will help to stabilize the micro droplets. As the increasing in the W/O ratio can dilute the concentration of the nanotubes in the suspension for a constant overall loading of nanotubes, more coalescence of the micro droplets occurred and bigger pores can be obtained finally. Besides the pore size, the distribution of the pores is also affected by the W/O ratio. Based on the optical images in Figure 4 (also Figure S5, Supporting Information), one can find that the increasing of W/O ratio also improve the uniformity of the pore

distribution, that is, the NPs distribution. Figure 4 (e) highlights the changes in the distribution of the nanotubes with the increasing of the W/O ratio. For a lower W/O ratio, a "fine but inhomogeneous" distribution of nanotubes coupled with smaller pores can be obtained, while, a high W/O ratio will give rise to a "coarse but homogeneous" distribution of the nanotubes. The significance of this change in the nanotube distribution has been shown by the W/O ratio dependent behavior of the electrical conductivity in Figure 4 (f). It can be found that the electrical conductivity increases with the W/O ratio, implying that a higher W/O ratio can effectively facilitate the formation of a continuous conductive pathway with the same amount of conductive nanofillers.

In addition to electrical conductivity, the thermal conductivity of the porous nanocomposites is worthy to be discussed. It has been reported that the increase in the porosity will remarkably reduce the thermal conductivity.[49] For the porous film with different W/O ratios, the higher the W/O ratio, the higher the porosity as indicated by the optical images since the porous structures are formed by the water phase. Therefore, a higher W/O ratio is favourable for the improvement of the thermoelectric figure of merit *ZT*, which is proportional to the product σ/k (σ, the electrical conductivity, k, the thermal conductivity) and the key parameter describing the properties of a thermoelectrical material. It is believed that the controllable porous structure coupled with the special distribution of NPs could provide an effective solution for achieving high electrical conductivity but low thermal conductivity, that is, a higher thermoelectric figure of merit *ZT*, which is very significant for thermoelectrical materials.

Conclusions

In summary, a tunable 3D network of nanoparticles in segregated nanocomposites via emulsion process has been realized for the first time. By individual design of the compositions of the water or oil phase in an emulsion system, the distribution and dispersion of nanoparticles can be well controlled in the resulting nanocomposites. The design flexibility for the compositions of the emulsion system combined with the simplicity of the fabrication of the nanocomposites will enable the manipulability of the distribution and dispersion of all the components as well as the structures, which is significant for development of advanced functional nanocomposites.

Acknowledgement

The author Dr. B. Geng appreciates the support from Shandong Provincial Education Department for his visiting Washington State University, and Dr. Zhong greatly acknowledges the support through the Washington State University Research Advancement Challenge (RAC) Grant.

Notes and references

[a] School of Chemistry and Chemical Engineering, University of Jinan, Jinan, 250022 (CHINA).
[b] School of Mechanical and Materials Engineering, Washington State University, Pullman, WA 99164 (USA).

[c] Department of Mechanical Engineering, Wichita State University, Wichita, KS 67260 (USA)
* Corresponding author: Katie_zhong@wsu.edu
[⊥] These authors contributed equally to this work.
Electronic Supplementary Information (ESI) available: Additional SEM and optical images as referenced in the text. See DOI: 10.1039/c000000x/

1. T. Kuilla, S. Bhadra, D. H. Yao, N. H. Kim, S. Bose and J. H. Lee, *Prog. Polym. Sci.*, 2010, **35**, 1350.
2. M. T. Byrne and Y. K. Gun'ko, *Adv. Mater.*, 2010, **22**, 1672.
3. F. Hussain, M. Hojjati, M. Okamoto and R. E. Gorga, *J. Compos. Mater.*, 2006, **40**, 1511.
4. Y. F. Li, J. H. Zhu, S. Y. Wei, J. E. Ryu, Q. Wang, L. Y. Sun and Z. H. Guo, *Macromol. Chem. Phys.*, 2011, **212**, 2429.
5. H. B. Gu, S. Tadakamalla, X. Zhang, Y. D. Huang, Y. Jiang, H. A. Colorado, Z. P. Luo, S. Y. Wei and Z. H. Guo, *Journal of Materials Chemistry C*, 2013, **1**, 729.
6. Q. He, T. Yuan, X. Zhang, S. Guo, J. Liu, J. Liu, X. Liu, L. Sun, S. Wei and Z. H. Guo, *Materials Research Express*, 2014, **1**, DOI: 10.1088/2053-1591/1/3/035029
7. M. C. de Jesus, R. A. Weiss and S. F. Hahn, *Macromolecules*, 1998, **31**, 2230.
8. H. Pang, T. Chen, G. M. Zhang, B. Q. Zeng and Z. M. Li, *Mater. Lett.*, 2010, **64**, 2226.
9. Y. Du, S. Z. Shen, K. F. Cai and P. S. Casey, *Prog. Polym. Sci.*, 2012, **37**, 820.
10. C. Yu, Y. S. Kim, D. Kim and J. C. Grunlan, *Nano Lett.*, 2008, **8**, 4428.
11. Y. R. Li, J. Chen, L. Huang, C. Li, J. D. Hong and G. Q. Shi, *Adv. Mater.*, 2014, **26**, 4789.
12. W. Li, Q. Yue, Y. H. Deng and D. Y. Zhao, *Adv. Mater.*, 2013, **25**, 5129.
13. A. Haryono and W. H. Binder, *Small*, 2006, **2**, 600.
14. P. S. K. Murthy, Y. M. Mohan, K. Varaprasad, B. Sreedhar and K. M. Raju, *J. Colloid Interface Sci.*, 2008, **318**, 217.
15. M. H. Al-Saleh, S. A. Jawad and H. M. Ghanem, *High Perform. Polym.*, 2014, **26**, 205.
16. M. C. Orilall and U. Wiesner, *Chem. Soc. Rev.*, 2011, **40**, 520.
17. H. Arora, Z. H. Li, H. Sai, M. Kamperman, S. C. Warren and U. Wiesner, *Macromol. Rapid Commun.*, 2010, **31**, 1960.
18. V. Kalra, J. Lee, J. H. Lee, S. G. Lee, M. Marquez, U. Wiesner and Y. L. Joo, *Small*, 2008, **4**, 2067.
19. S. C. Warren, L. C. Messina, L. S. Slaughter, M. Kamperman, Q. Zhou, S. M. Gruner, F. J. DiSalvo and U. Wiesner, *Science*, 2008, **320**, 1748.
20. V. Raman, A. Bose, B. D. Olsen and T. A. Hatton, *Macromolecules*, 2012, **45**, 9373.
21. Y. J. Gao, Z. Y. Liu, C. L. Yin, S. L. Huang and M. B. Yang, *Polym. Adv. Technol.*, 2012, **23**, 695.
22. C. L. Yin, Z. Y. Liu, Y. J. Gao and M. B. Yang, *Polym. Adv. Technol.*, 2012, **23**, 1112.
23. Q. Y. Zhang, Z. Fang, Y. Cao, H. M. Du, H. Wu, R. Beuerman, M. B. Chan-Park, H. W. Duan and R. Xu, *Acs Macro Letters*, 2012, **1**, 876.
24. P. S. Gils, D. Ray and P. K. Sahoo, *Int. J. Biol. Macromol.*, 2010, **46**, 237.
25. Q. B. Wie, Y. L. Luo, F. Fu, L. J. Gao and Y. W. Song, *Colloid J.*, 2013, **75**, 34.
26. J. C. Grunlan, A. R. Mehrabi, M. V. Bannon and J. L. Bahr, *Adv. Mater.*, 2004, **16**, 150.
27. D. Kim, Y. Kim, K. Choi, J. C. Grunlan and C. H. Yu, *Acs Nano*, 2010, **4**, 513.
28. N. Cohen, D. C. Samoocha, D. David and M. S. Silverstein, *J. Polym. Sci., Part A: Polym. Chem.*, 2013, **51**, 4369.
29. Y. Bao, L. Xu, H. Pang, D. X. Yan, C. Chen, W. Q. Zhang, J. H. Tang and Z. M. Li, *J. Mater. Sci.*, 2013, **48**, 4892.
30. H. Pang, C. Chen, Y. Bao, J. Chen, X. Ji, J. Lei and Z. M. Li, *Mater. Lett.*, 2012, **79**, 96.
31. A. Ameli, M. Nofar, C. B. Park, P. Potschke and G. Rizvi, *Carbon*, 2014, **71**, 206.

32. A. Ameli, P. U. Jung and C. B. Park, *Carbon*, 2013, **60**, 379.

33. A. Ameli, P. U. Jung and C. B. Park, *Compos. Sci. Technol.*, 2013, **76**, 37.

34. U. T. Gonzenbach, A. R. Studart, E. Tervoort and L. J. Gauckler, *Angew. Chem.-Int. Edit.*, 2006, **45**, 3526.

35. S. Tcholakova, N. D. Denkov and A. Lips, *Phys. Chem. Chem. Phys.*, 2008, **10**, 1608.

36. B. P. Binks and C. P. Whitby, *Colloids and Surfaces a-Physicochemical and Engineering Aspects*, 2005, **253**, 105.

37. A. R. Studart, H. C. Shum and D. A. Weitz, *J. Phys. Chem. B*, 2009, **113**, 3914.

38. W. Liu, L. J. Du, Y. Z. Wang, J. L. Yang and H. Xu, *Ceram. Int.*, 2013, **39**, 8781.

39. J. Huo, M. Marcello, A. Garai and D. Bradshaw, *Adv. Mater.*, 2013, **25**, 2717.

40. A. Menner, R. Verdejo, M. Shaffer and A. Bismarck, *Langmuir*, 2007, **23**, 2398.

41. L. L. C. Wong, S. Barg, A. Menner, P. D. Pereira, G. Eda, M. Chowalla, E. Saiz and A. Bismarck, *Polymer*, 2014, **55**, 395.

42. S. Livshin and M. S. Silverstein, *Macromolecules*, 2008, **41**, 3930.

43. Y. Lumelsky and M. S. Silverstein, *Macromolecules*, 2009, **42**, 1627.

44. T. N. Hunter, R. J. Pugh, G. V. Franks and G. J. Jameson, *Adv. Colloid Interface Sci.*, 2008, **137**, 57.

45. R. Aveyard, B. P. Binks and J. H. Clint, *Adv. Colloid Interface Sci.*, 2003, **100**, 503.

46. T. M. Wu, E. C. Chen, Y. W. Lin, M. F. Chiang and G. Y. Chang, *Polym. Eng. Sci.*, 2008, **48**, 1369.

47. S. Abbasi, P. J. Carreau, A. Derdouri and M. Moan, *Rheol. Acta*, 2009, **48**, 943.

48. S. Abbasi, A. Derdouri and P. J. Carreau, *Polym. Eng. Sci.*, 2011, **51**, 992.

49. L. Braginsky, V. Shklover, G. Witz and H. P. Bossmann, *Physical Review B*, 2007, **75**, 094301.

Figure 1. Fabrication of the porous nanocomposites with controlled dispersion and distribution of nanoparticles. (a) Preparation of emulsion of polymer solution/NPs suspension by ultrasonication, (b) Schematic of the compositions/structures of the emulsion, (c) digital photo of the porous nanocomposite film after drying, and SEM images of the surface (contacted with the substrate) (d) and fracture surface (e) of the porous film. Scale bars: (d) 100μm, (e) 10μm. (f) Schematic of the controlled distribution of NPs (MWCNT, for example). For details, see the text.

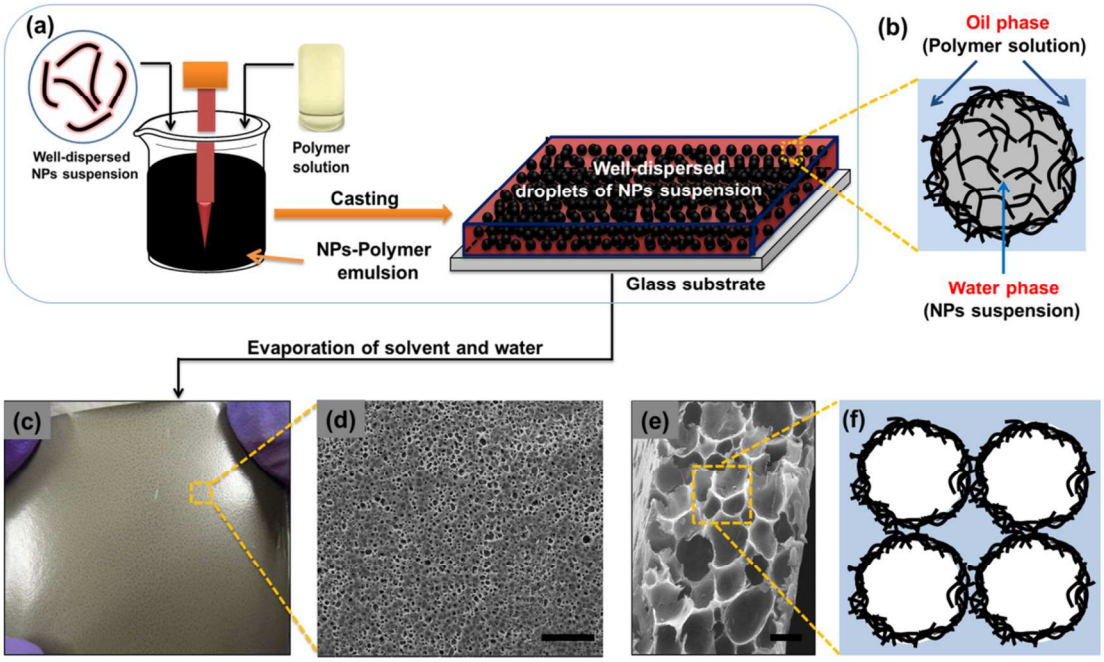

Figure 2. (a) CNT loading dependent behavior of the electrical properties of the porous film (the cartoon shows the mechanism for the formation of the conduction percolation); (b) Optical image for the conductive network constructed by the porous structures and (c) SEM images showing the distribution of NPs on the surface of the pores

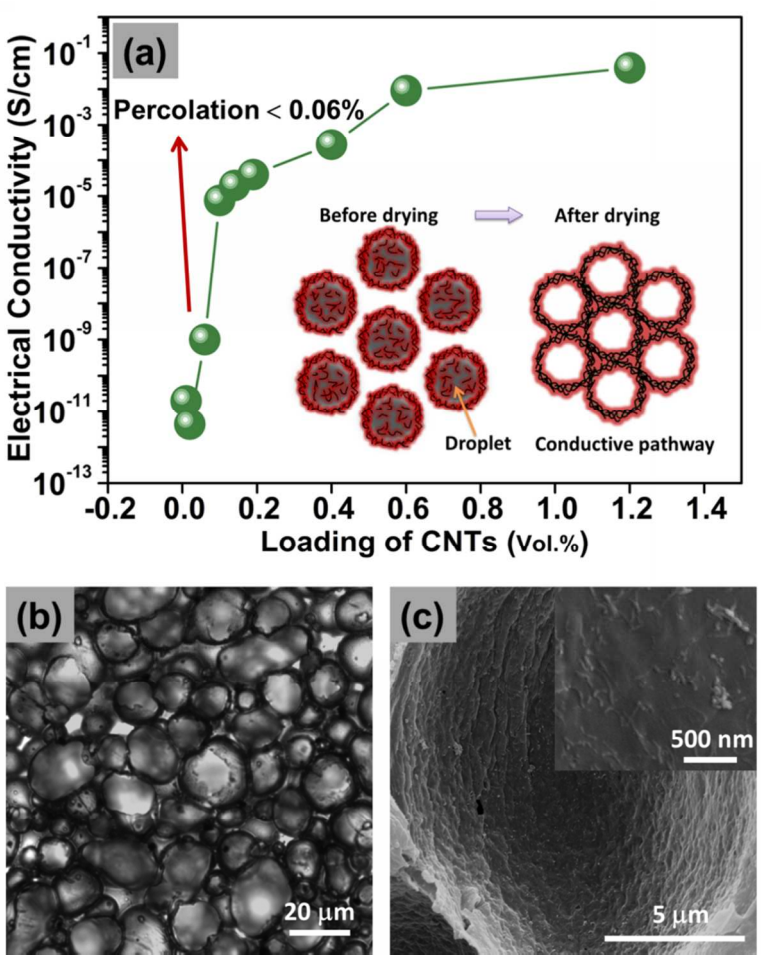

Figure 3. Effects of NPs loading on the distribution of NPs as revealed by the pore diameter (a fixed W/O ratio of 0.15 was used for all the concentrations). (a) – (e): the SEM images of the fracture surface showing the pore structures with increasing loading of MWCNTs as indicated in (f), the diameter of the pores as a function of MWCNTs loading (scale bars: 50 μm)

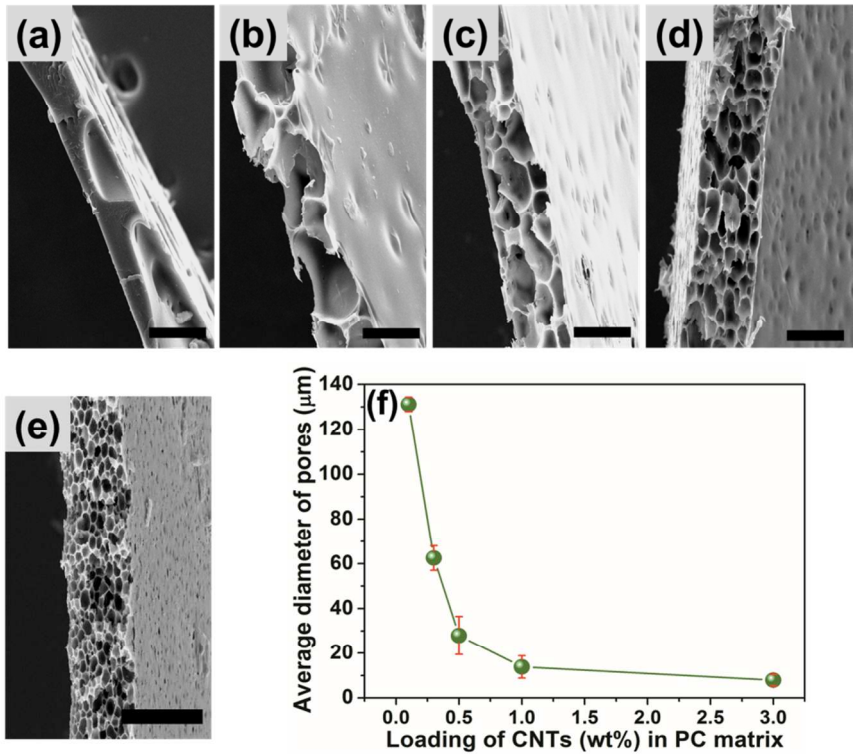

Figure 4. Control the distribution of NPs (pore structures) by varying the W/O volume ratio (the overall loading of MWCNT is 2 wt%) as revealed by optical images: (a) 0.05, (b) 0.15, (c) 0.2 and (d) 0.3 (scale bars: 20 μm). (e) Schematic of the effects of W/O ratio on the distribution of NPs and (f), the distribution state dependent behavior of the electric conductivity.